

# Silencing of the small GTPase DIRAS3 induces cellular senescence in human white adipose stromal/progenitor cells

Asim Ejaz<sup>1</sup>, Monika Mattesich<sup>2</sup>, Werner Zwerschke<sup>1</sup>

<sup>1</sup> Division of Cell Metabolism and Differentiation Research, Institute for Biomedical Aging Research, University of Innsbruck, A-6020 Innsbruck, Austria

<sup>2</sup> Department of Plastic and Reconstructive Surgery, Innsbruck Medical University, A-6020 Innsbruck, Austria

**Correspondence to:** Werner Zwerschke; **email:** [werner.zwerschke@uibk.ac.at](mailto:werner.zwerschke@uibk.ac.at)

**Keywords:** adipose stem cell, adipose stromal/progenitor cell, adipocyte, adipogenesis, aging, DIRAS3, mTOR, obesity, senescence

**Received:** November 2, 2016

**Accepted:** March 3, 2017

**Published:** March 17, 2017

## ABSTRACT

Inhibition of Akt-mTOR signaling protects from obesity and extends life span in animals. In the present study, we analyse the impact of the small GTPase, GTP-binding RAS-like 3 (DIRAS3), a recently identified weight-loss target gene, on cellular senescence in adipose stromal/progenitor cells (ASCs) derived from human subcutaneous white adipose tissue (sWAT). We demonstrate that DIRAS3 knock-down (KD) in ASCs induces activation of Akt-mTOR signaling and proliferation arrest. DIRAS3 KD ASCs lose the potential to form colonies and are negative for Ki-67. Moreover, silencing of DIRAS3 results in a premature senescence phenotype. This is characterized by senescence-associated  $\beta$ -galactosidase positive enlarged ASCs containing increased p16<sup>INK4A</sup> level and activated retinoblastoma protein. DIRAS3 KD ASCs form senescence-associated heterochromatic foci as shown by increased level of  $\gamma$ -H2A.X positive foci. Furthermore, these cells express a senescence-associated secretory phenotype characterized by increased interleukin-8 secretion. Human DIRAS3 KD ASCs develop also a senescence phenotype in sWAT of SCID mice. Finally, we show that DIRAS3 KD in ASCs stimulates both adipogenic differentiation and premature senescence. In conclusion, our data suggest that silencing of DIRAS3 in ASCs and subsequently hyper-activation of Akt-mTOR drives adipogenesis and premature senescence. Moreover, differentiating ASCs and/or mature adipocytes may acquire features of cellular senescence.

## INTRODUCTION

Obesity is a major public-health problem worldwide. Underlying cause of this epidemic is the inherent expansion and renewal capacity of adipocytes, which differentiate from adipose stromal/progenitor cells (ASCs) in a process referred to as adipogenesis [1-3]. ASCs derived from the stromal-vascular fraction (SVF) of white adipose tissue (WAT) are multipotent and can differentiate *in vitro* into several lineages [2, 4, 5]. Adipogenesis involves ASC determination and terminal differentiation into adipocytes, which express fat cell specific genes and accumulate lipids [6, 7]. This process is governed by a complex signal transducing network including Delta-like protein 1/Preadipocyte factor 1-, Wnt-, insulin-, IGF-1-signaling and numerous additional pathways, which eventually activate or

repress a cascade of adipogenic transcription factors. Most central in this cascade are members of the CCAAT/enhancer-binding protein (C/EBP) family and the nuclear receptor peroxisome proliferator-activated receptor- $\gamma$ 2 (PPAR $\gamma$ 2). Weight-loss (WL) leads to a reduction in the size of adipocytes. This is associated with endocrine and metabolic benefits [8]. Health-promoting effects of WL exceed however those directly associated with reduction of adipocyte size and fat mass [9]. Increasing evidence suggest beneficial effects of WL on ASCs [10, 11]. We have recently demonstrated that WL leads to upregulation of the small GTPase, GTP-binding RAS-like 3 (DIRAS3) [12, 13], in ASCs of human subcutaneous (s) WAT [14]. DIRAS3 negatively regulates adipogenesis via inhibition of Akt-mechanistic target of rapamycin (mTOR) signaling in the ASCs [14]. Akt-mTOR signaling is well-known as

positive regulator of adipogenesis and inhibition of this pathway protects from obesity [15]. This underscores the role of DIRAS3 as WL target gene.

Obesity is associated with an increased number of senescent ASCs [16, 17]. Reduced Akt-mTOR signaling decreases cellular senescence [18] and induces lifespan extension in animal models [15]. We have previously shown that long-term WL postpones replicative senescence in human ASCs [10]. Whether the WL target gene DIRAS3 is involved in regulation of proliferation and senescence in ASCs is unknown. Cellular senescence plays an important role in tumor suppression and organismal aging and emerging evidence suggest additional relevance in development, tissue remodeling and repair [19]. Cellular senescence results in terminal cell cycle arrest eventually induced by up-regulation of the cell cycle inhibitors p16<sup>INK4A</sup> and p21<sup>CIP1</sup> and represents phenotypically diverse cellular states, which are characterized by distinct morphological and biochemical alterations [19]. The senescence program can be induced by various cell-intrinsic and -extrinsic stress stimuli, for example DNA damage, oncogene assault induced by activation of oncogenes [20] or loss of tumor suppressors [21] and inflammation [22]. In aged tissues, including sWAT, senescent cells accumulate, which exacerbate dysfunction and contribute to the aging phenotype [16, 23]. Ablation of senescent cells in aged sWAT of mice alleviates age-related dysfunctions [24-26]. These findings underscore the importance of cellular senescence in adipose tissue aging and are reflected by progenitor cell populations isolated from adipose depots of older donors, which exhibit impaired replicative and adipogenic capacity and contain senescent cells [25, 27-29]. The mechanisms underlying senescence in ASCs are however not precisely understood. In the present study, we investigated the influence of DIRAS3 on cellular senescence and proliferative capacity of ASCs of the human sWAT.

## RESULTS

### DIRAS3 suppresses hyper-activation of Akt-mTOR pathway and sustains proliferation of human ASCs

To investigate the effect of DIRAS3 knock-down (KD) on Akt-mTOR signaling in ASCs we employed lentivirus mediated DIRAS3 specific shRNA (Fig. 1A and [14]). DIRAS3 KD leads to increased activity of Akt-mTOR signaling in ASCs (Fig. 1B). As mTOR activity is essential for cell proliferation but a persistent mTOR complex 1 activation leads to exhaustion of stem cells [18, 30], we investigated the effect of DIRAS3 KD on proliferation of ASCs. We found that DIRAS3 KD abrogates ASC proliferation (Fig. 2A – 2C). This effect

was dose-dependent (Supplementary Fig. S1A). We observed a significantly lower colony formation index upon DIRAS3 KD in colony-formation assays (Fig. 2D and 2E). Upon DIRAS3 KD, we detected a strong decrease in the expression of proliferation marker Ki-67, which is expressed in all phases of the cell cycle except G0 (Fig. 2F). We detected neither an increased number of floating cells nor significant difference in percentage of apoptotic cells upon DIRAS3 KD in annexin V/propidium iodide staining assays (Supplementary Fig. S1B), indicating that the lower number of cells and colonies observed upon DIRAS3 KD is not due to increased apoptosis. Together these results indicate that a certain level of DIRAS3 is necessary to suppress hyper-activation of Akt-mTOR pathway and to sustain proliferation, suggesting that DIRAS3 contributes in maintaining self-renewal capacity of the human ASCs.

### DIRAS3 KD induces premature senescence in human ASCs

DIRAS3 KD cells displayed a cytoplasm with thin and long processes and a significant number of these cells became flat (Fig. 3A and 3B), resembling the morphological features of the premature senescence phenotype induced by oncogenic assault in primary human fibroblasts [20]. As demonstrated by cytochemical staining (Fig. 3B and 3C) and FACS analyses using a fluorogenic substrate C<sub>12</sub>FDG (Supplementary Fig. S2A), DIRAS3 KD led to a significant increase in the number of senescence-associated  $\beta$ -galactosidase (SA- $\beta$ -GAL) positive ASCs and to a significant increase in cell size (Supplementary Fig. S2B). To assess the involvement of DNA damage response (DDR) in DIRAS3 KD induced premature senescence, we analysed formation of senescence-associated heterochromatic foci (SAHF) using immunofluorescence staining and observed higher specific foci in DIRAS3 KD cells (Supplementary Fig. S2C). In addition, we detected a significant higher level of phosphorylated (ser139)  $\gamma$ -H2A.X protein by western blotting in cell lysates from DIRAS3 KD ASCs compared to shCntrl transduced ASCs (Fig. 3D). Cellular senescence can mainly be induced by activation of either p53/p21CIP1, p16INK4A/Retinoblastoma protein (Rb) or both pathways depending on the nature and magnitude of stress [19]. We detected significant higher levels of phosphorylated (ser15) p53 upon DIRAS3 KD in the ASCs (Fig. 3E), indicating activation of the p53 pathway. Although we found slightly higher p21CIP1 mRNA expression in DIRAS3 KD ASCs relative to shCntrl cells (Supplementary Fig. S2D), we have not observed a significant change in the p21CIP1 protein level (Fig. 3E). This suggests a relatively weak activation of the

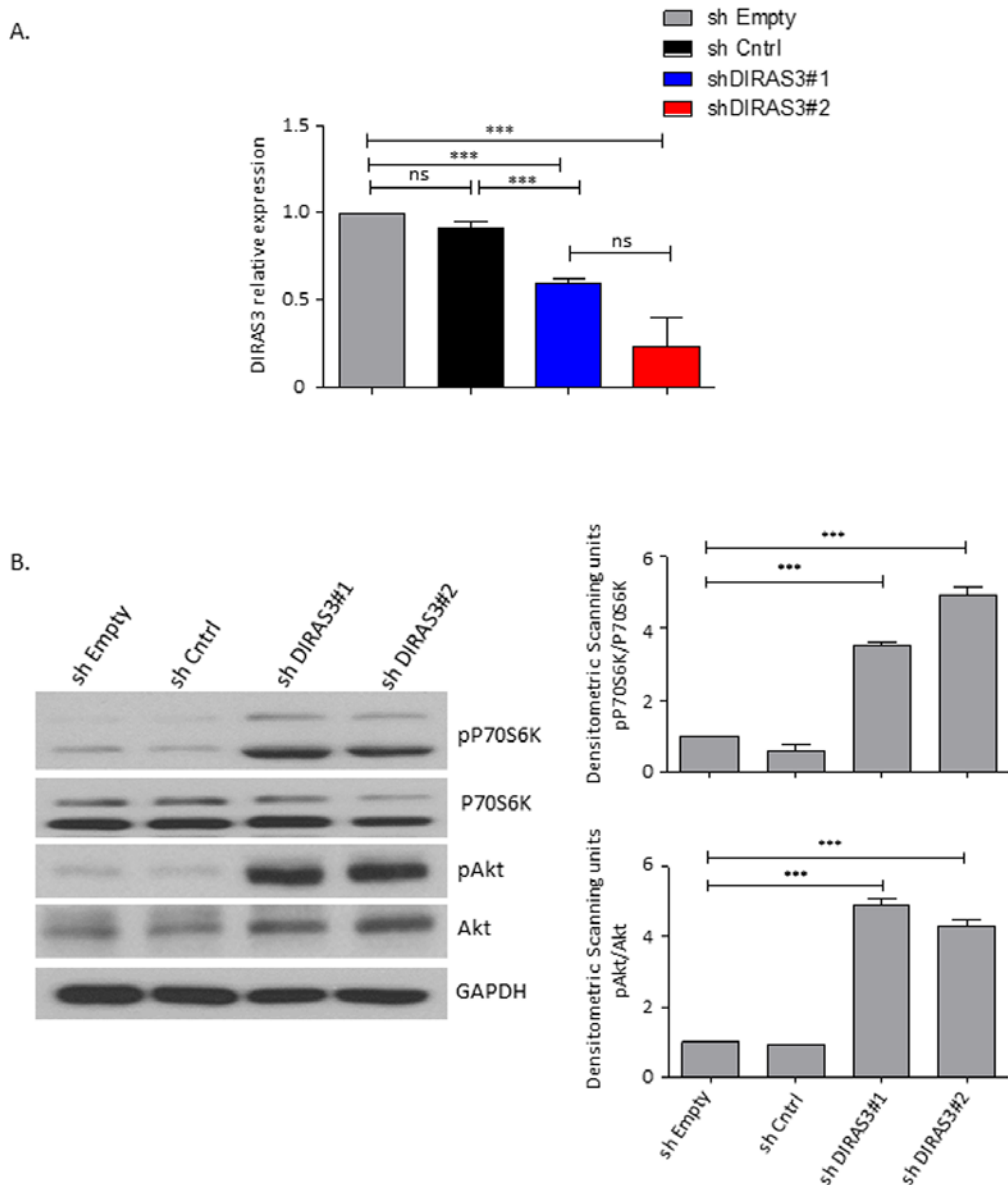


**Figure 1. DIRAS3 knock-down (KD) leads to an upregulation of Akt-mTOR signalling in proliferating ASCs.** (A) Efficiency of DIRAS3 KD in ASCs. DIRAS3 mRNA levels were measured by quantitative real time PCR (q-RT PCR) following infection of ASCs with lentiviruses expressing DIRAS3 specific shRNA. An empty vector control (shEmpty) and a scrambled sh sequence (shCntrl) are employed as controls (n=4). (B) Activation of Akt and p70S6K by DIRAS3 KD in ASCs. (Left panel) DIRAS3 was KD in ASCs using specific shRNAs as indicated. Cells were starved by serum withdrawal for 48 hours. Afterwards cell lysates were prepared and phosphorylation of Akt (S473) and P70S6K (T389) was examined by immune-blotting using specific antibodies. GAPDH served as an input control. (Right panels) Fold changes in densitometric band intensities presented as Arbitrary Units (AU) for phosphorylated proteins normalized to un-phosphorylated total proteins, acquired by image J were compared. Band intensity of shCntrl 0% FCS was taken as 1. Western blot shown is from replicate from one donor with similar protein expression pattern was observed with 2 different donors. All error bars represents the means  $\pm$  SEM. p values \* =  $p < 0.05$ , \*\* =  $p < 0.001$  and \*\*\* =  $p < 0.0001$ .

p53/p21CIP1 arm in DIRAS3 KD induced cellular senescence (DICS) in cultured human ASCs. While, we detected a very strong induction of p16INK4A at both mRNA and protein level in DIRAS3 KD ASCs (Fig. 3E and Supplementary Fig. S2E). Both cyclin-dependent

kinase inhibitors (CDKI's), p21CIP1 and p16INK4A, induce proliferation arrest via the inhibition of G1/S CDKs. This leads to activation of cell cycle break Rb by reduced phosphorylation. We analyzed whether DIRAS3 KD leads to reduced Rb phosphorylation. We

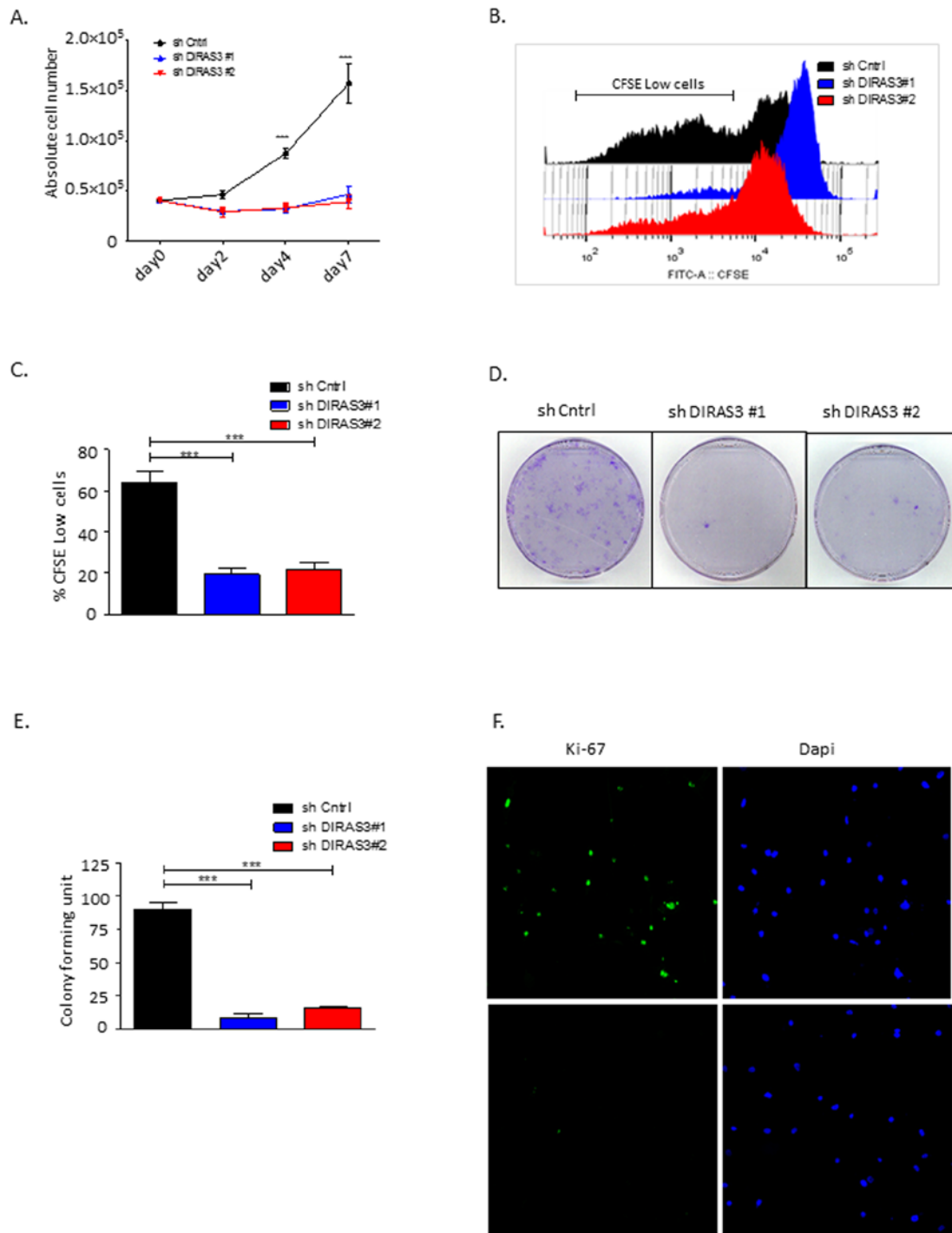


**Figure 2. Silencing of DIRAS3 reduces proliferation and self-renewal of human ASCs.** (A) Proliferation of ASCs following knock-down (KD) of DIRAS3 was monitored by cell counting (n=4). (B and C) Monitoring of cell proliferation by CFSE signal dilution technique. Flow cytometric analyses demonstrated a higher proliferation rate of shCntrl relative to shDIRAS3 infected ASCs, reflected by a significantly higher percentage of CFSE low cells compared to shDIRAS3 infected ASCs. Differentially transduced ASCs were stained with CFSE and cultured for 4 days. Dilution of CFSE signal was monitored by FACS (B). Percentage of CFSE low cells was plotted (C) (n=4). (D and E) ASCs were seeded at a density of 500 cells in tissue culture dish following transduction with shDIRAS3 and shCntrl expressing lentiviruses and selection. Number of colonies were counted 10 days post seeding after staining with crystal violet (D) and plotted (E) (n=3) (F) Expression of Ki-67 was assessed in transduced ASCs via confocal microscopy. Cells were fixed on cover slips and stained for Ki-67 (green) and DAPI (blue) for nuclear staining (n=3). All error bars represents the means  $\pm$  SEM. p values \*\*\* =  $p < .0001$ .

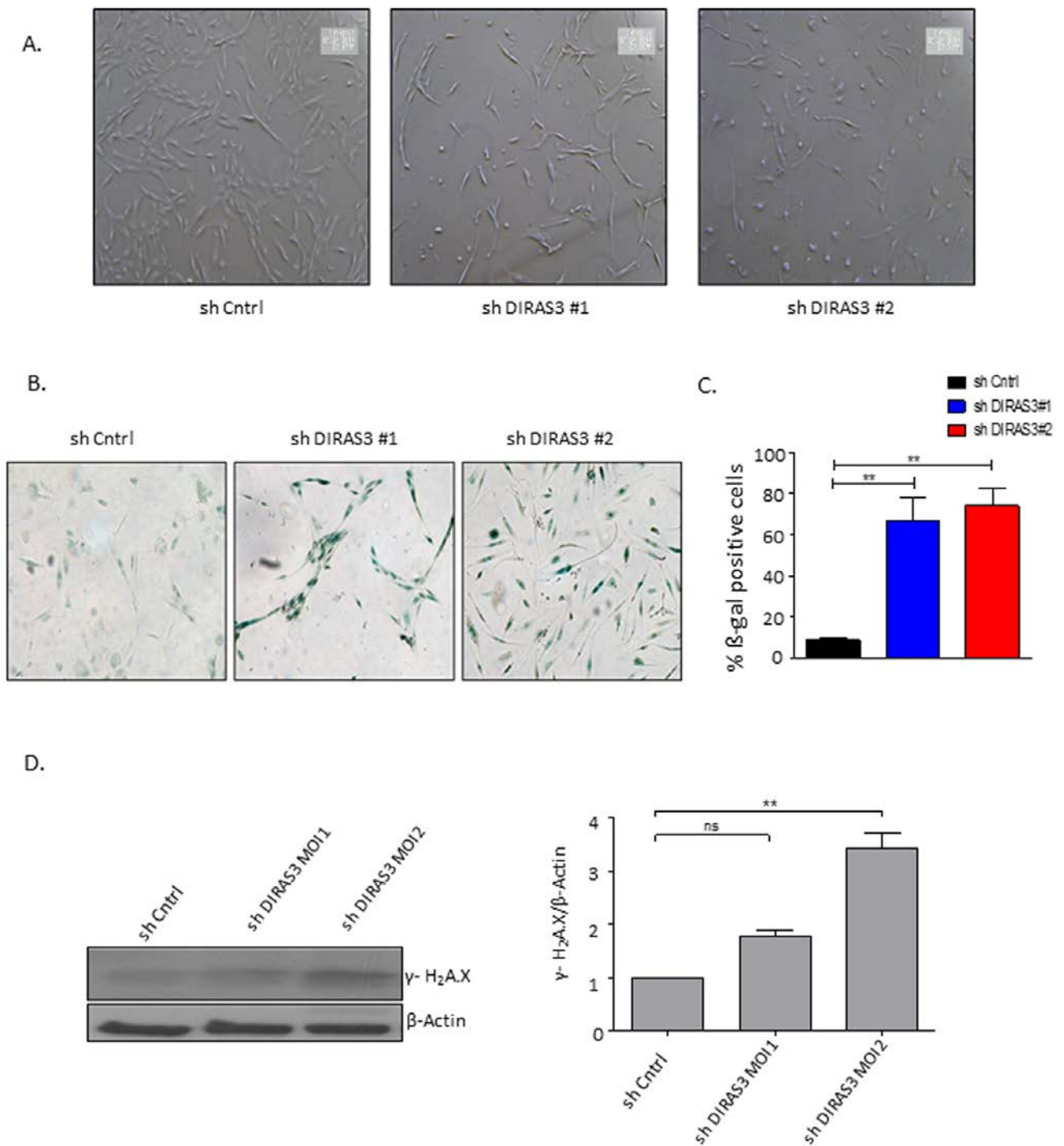


**Figure 3. Silencing of DIRAS3 induces premature senescence in human ASCs.** (A) Morphology of ASCs infected with shCntrl and shDIRAS3 was documented using light microscope at 40x magnification. (B and C) ASCs infected with either shDIRAS3 or shControl (shCntrl) expressing lentiviruses were fixed and stained for SA- $\beta$ -GAL. Percentage of SA- $\beta$ -GAL positive cells was calculated by scanning 5 low-power magnification fields (n=3). (D) ASCs were transduced by indicated lentiviruses with increasing MOI and cell lysates immunoblotted using phospho-Ser-139 Gamma H2A.X antibody.  $\beta$ -Actin served as a loading control.

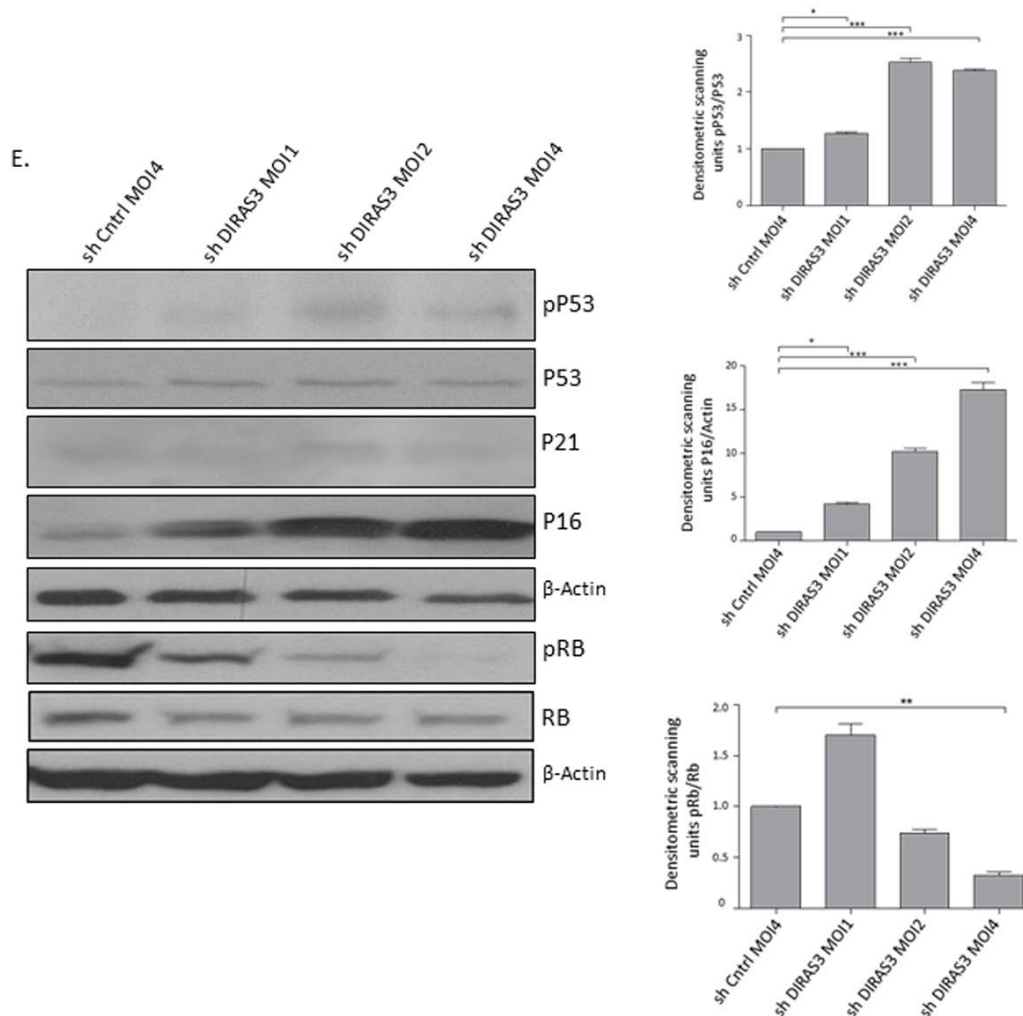


**Figure 3E (Continues). Silencing of DIRAS3 induces premature senescence in human ASCs.** DIRAS3 was KD in ASCs using lentiviruses expressing specific shRNA at increasing MOI. Cell lysates were immunoblotted with the specific antibodies to investigate accumulation of senescent associated proteins p16<sup>INK4A</sup>, p21<sup>CIP1</sup>, p53 phosphorylated p53 (S15), Rb and pRb (S807/811).  $\beta$ -Actin served as a loading control. Fold changes in densitometric band intensities for phosphorylated proteins normalized to un-phosphorylated total proteins, acquired by image J were compared. Band intensity of shCntrl was taken as 1. Western blot shown is from replicate from one donor with similar protein expression pattern was observed with 2 different donors. All error bars represents the means  $\pm$  SEM. p values \* =  $p < 0.05$ , \*\* =  $p < 0.001$  and \*\*\* =  $p < 0.0001$ .

observed a significant decrease in serine 807/811 phosphorylated Rb in DIRAS3 KD ASCs (Fig. 3E), suggesting that DIRAS3 KD induces proliferation arrest by abrogating Rb phosphorylation.

#### DIRAS3 KD ASCs develop a senescence-associated secretory phenotype

To analyse whether DIRAS3 KD ASCs show features of the senescence-associated secretory phenotype (SASP) we measured the expression of interleukin 6 (IL-6), IL-8, IL-1 $\beta$  and TNF  $\alpha$  genes coding for secreted factors which are frequently upregulated in senescent

cells [31]. Results revealed a strong up-regulation of IL-8 mRNA expression (Fig. 4A) while the expression of the other genes was not increased. PCR data were verified by quantitative ELISA (Fig. 4B) and FACS analysis (Fig. 4C and 4D), showing increased IL-8 staining in DIRAS3 KD ASCs and increased secretion of the pro-inflammatory cytokine from these cells. Acosta et al., 2008 [22] have shown that senescent cells activate a self-amplifying secretory program in which ligands of the IL-8 receptor (CXCR2) reinforce growth arrest. To strengthen the results we analysed CXCR2 expression. We observed a significant increase in the expression of CXCR2, in DIRAS3 KD cells (Fig. 4E).

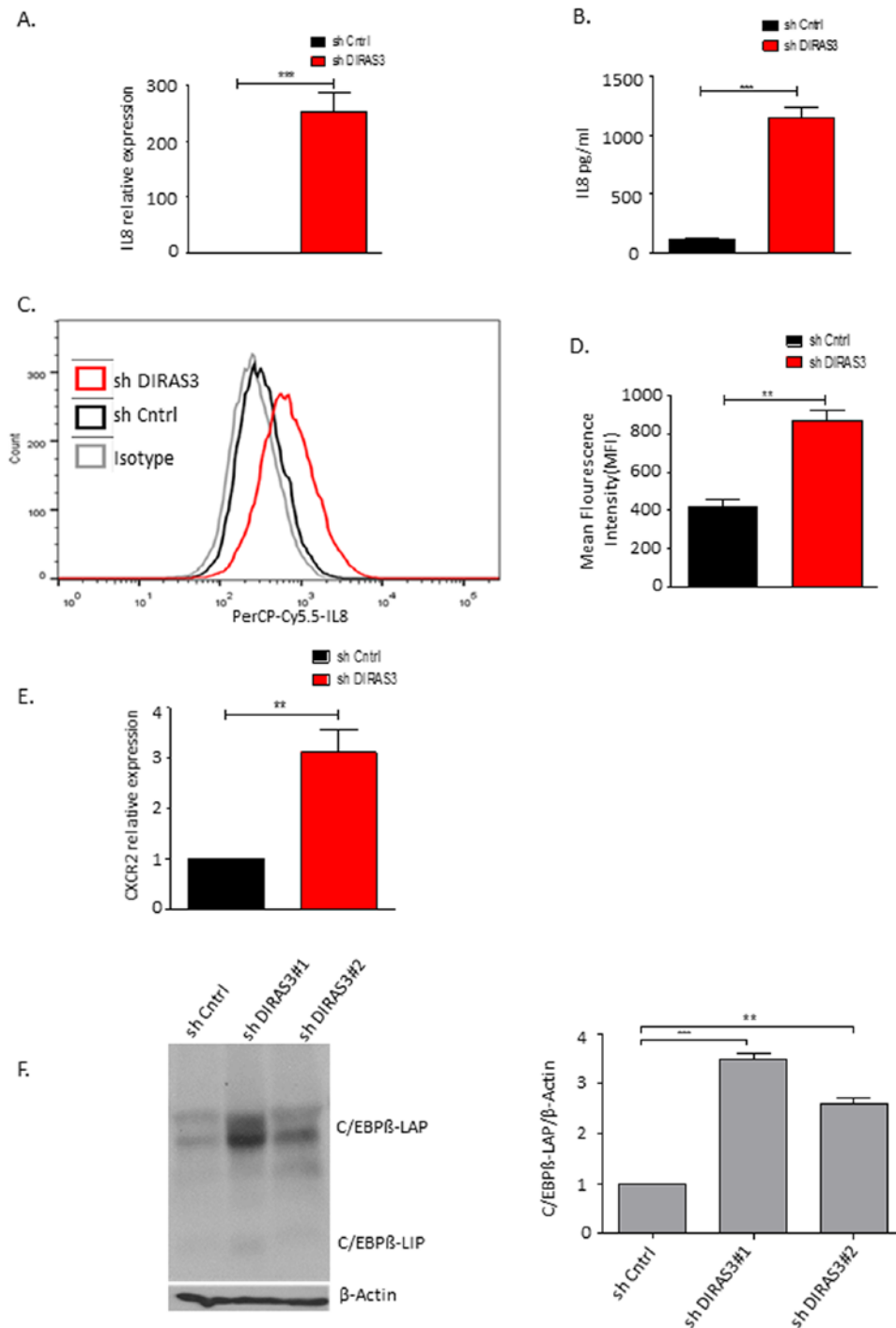


**Figure 4. DIRAS3 KD induced senescence lead to higher production of IL-8.** (A) IL-8 mRNA was quantified using q-RT PCR upon DIRAS3 KD (n=4). (B) IL-8 protein level in cell culture supernatant was quantified by ELISA (n=3). (C and D) Differentially transduced ASCs were incubated for 4 hours with brefeldin A (5µg/ml) – a protein transport inhibitor from Endoplasmic reticulum to Golgi complex, followed by fixation and permeabilization. Cells were stained by PerCP-Cy5.5-IL-8 antibody and analyzed by FACS (n=2). (E) CXCR2 mRNA was quantified using q-RT PCR upon DIRAS3 KD (n=4) (F) (Left panel) C/EBPβ protein level upon KD of DIRAS3 was analyzed by immune-blotting using anti-C/EBPβ antibodies. β-Actin served as input control. (Right panel) Fold changes in densitometric band intensities for phosphorylated proteins normalized to un-phosphorylated total proteins, acquired by image J were compared. Band intensity of shCntrl was taken as 1. Western blot shown is from replicate from one donor with similar protein expression pattern was observed with 2 different donors. All error bars represents the means ± SEM. p values \* = p<0.05, \*\* = p<0.001 and \*\*\* = p<.0001.

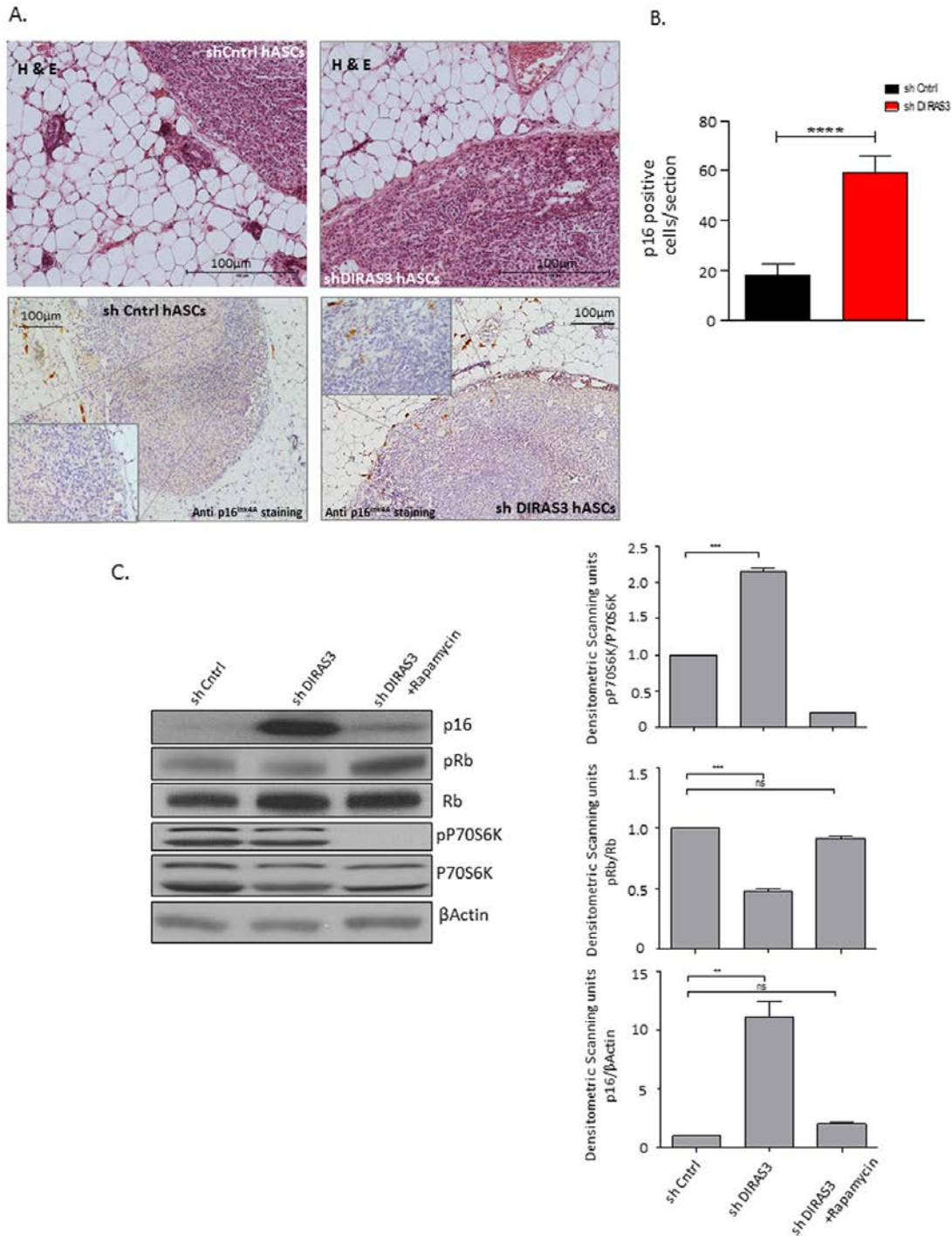


**Figure 5. Human DIRAS3 KD ASCs develop a senescence phenotype in posterior SWAT of SCID mice.** (A) (Upper panel) Human shDIRAS3 ASCs (shDIRAS3 hASCs) and shCtrl hASCs were xenotransplanted into posterior SWAT of SCID mice. Injection sites of hASCs were histologically identified and marked by H&E staining. (Lower panel) Senescent DIRAS3 KD hASCs were detected by immunohistochemical staining using anti p16<sup>INK4A</sup> antibodies. Region of Interest (ROI) is shown in higher magnification. (B) Number of p16<sup>INK4A</sup> positive hASCs per section were counted and plotted (n = 5 per group). (C) (Left panel) Cell lysates from control ASCs and DIRAS3 KD ASCs cultured with and without 20 nM rapamycin were blotted for p16<sup>INK4A</sup>, Rb, pRb (S807/811), P70S6K and pP70S6K (T389) using specific antibodies. β-Actin served as loading control. Note, rapamycin was added 2 days after virus infection. (Right panels) Fold changes in densitometric band intensities presented as Arbitrary Units (AU) for phosphorylated proteins normalized to un-phosphorylated total proteins, acquired by image J were compared. Band intensity of shCtrl was taken as 1 (n=2). All error bars represents the means ± SEM. p values \* = p<0.05, \*\* = p<0.001 and \*\*\* = p<0.0001.



Mechanistically an up-regulation of C/EBP $\beta$  was shown to play a critical role in OIS related induction of IL-8 [22]. Similarly, we found that C/EBP $\beta$  protein level is up-regulated in DIRAS3 KD ASCs (Fig. 4F).

### **Human DIRAS3 KD ASCs develop a senescence phenotype in posterior sWAT of SCID mice**

Since a DIRAS3 ortholog does not exist in mice [12], we analysed the *in vivo* relevance of DICS in a SCID mouse xenograft model. DIRAS3 KD and shCntrl human ASCs were injected into the posterior sWAT of SCID mice and tissue sections harboring the injection site were stained by immunohistochemistry for p16<sup>INK4A</sup> at six weeks post-injection. Analyses revealed a significant higher number of p16<sup>INK4A</sup> positive cells in mice injected with shDIRAS3 transduced ASCs (Fig. 5A and 5B), suggesting that DIRAS3 KD induces senescence in human ASCs in sWAT of mammals. To finally validate our hypothesis that DIRAS3 KD induced hyperactivity of mTOR leads to p16<sup>INK4A</sup> induction and hence premature senescence, we down-modulated mTOR activity in DIRAS3 KD ASCs using rapamycin. Western blot analyses revealed that rapamycin treatment rescued DIRAS3 KD induced p16<sup>INK4A</sup> up-regulation and Rb phosphorylation thus supporting our hypothesis (Fig. 5C).

### **Silencing of DIRAS3 in ASCs induces both adipogenic differentiation and premature senescence**

We have recently demonstrated that silencing of DIRAS3 induces adipogenic differentiation in ASCs via activation of Akt-mTOR signaling [14]. DIRAS3 KD strongly activated this signaling pathway and facilitated adipogenesis in ASCs treated with differentiation hormone cocktail. In the present study, we show that DIRAS3 KD mediated activation of Akt-mTOR signaling induces proliferation arrest and premature senescence in normal proliferating ASCs. To better understand the relationship between the role of DIRAS3 in regulation of senescence and adipogenesis we induced adipogenic differentiation in DIRAS3 KD ASCs and analysed senescence, adipogenesis and adipocyte markers 3 and 9 days after induction of differentiation. As shown before, silencing of DIRAS3 enhanced the induction of adipocyte differentiation as demonstrated by a higher number of cells staining positive by Oil-Red-O staining (Fig. 6A). Furthermore, we observed a significant up-regulation of the expression of the key adipogenic transcription factor PPAR $\gamma$ 2 and the adipocyte markers FABP4 and perilipin (Fig. 6B). Moreover, the level of the major adipocyte marker protein perilipin was increased in the resulting adipocytes (Fig. 6C and 6D). Intriguingly, DIRAS3 KD resulted also in strong upregulation of the

major senescence marker p16<sup>INK4A</sup> at mRNA (Fig. 6F) and protein level (Fig. 6C and 6E) in the resulting DIRAS3 KD adipocytes. Furthermore, p16<sup>INK4A</sup> protein was also detectable in *in vitro* differentiated adipocytes arising from wild type ASCs (Fig. 6C). Double staining experiments of *in vitro* differentiated adipocytes arising from ASCs 14 days after induction of adipogenic differentiation showed that these cells are SA- $\beta$ -galactosidase positive and contain Oil-Red-O stained fat droplets (Supplementary Fig. S3). In conclusion, these data indicate that silencing of DIRAS3 in human ASCs stimulates both adipogenic differentiation and premature senescence. Moreover, our data suggest that wild type adipocytes per se show features of cellular senescence.

## **DISCUSSION**

Deterioration of sWAT is a common feature with advancing age [27, 32]. The age-related detrimental changes in adipose tissue are not well understood. The current model suggests that accumulation of senescent adipose progenitors in aged WAT, which exacerbate dysfunctions and loss of fat mass, contributes to this aging phenotype [16, 23-26]. Adipose tissue is also a site of senescent cell accumulation in obesity [16,17]. In fact, while the ASC pool capable of self-renewal and differentiation is essential for homeostasis, regeneration, expansion and, hence functional maintenance of WAT, ASC populations isolated from adipose depots of aged or obese donors exhibit impaired replicative and adipogenic capacity and contain senescent cells [10, 16, 17, 25, 29].

Little is known regarding the molecular mechanisms underlying cellular senescence in ASCs. We recently identified the small GTPase, DIRAS3, a well characterized tumor suppressor protein [13], as a WL target gene in ASCs of human sWAT and show that DIRAS3 negatively regulates adipogenesis [14]. In the present study, we showed for the first time that silencing of DIRAS3 induces cell cycle arrest and premature senescence in ASCs by hyperactivation of mTOR. Our results indicate that this leads eventually to premature senescence by strong activation of the p16<sup>INK4A</sup>/Rb pathway and to a lesser extent of the p53/p21<sup>CIP1</sup> pathway. DDR likely contributes to this senescence phenotype, as DIRAS3 KD ASCs showed an increased number of foci containing the phosphorylated form of histone H2AX, a marker of DNA damage.

Studies support the hypothesis that signaling pathways that induce stem/progenitor cell growth, and hence transient amplification, contribute to stem cell exhaustion and depletion when aberrantly or

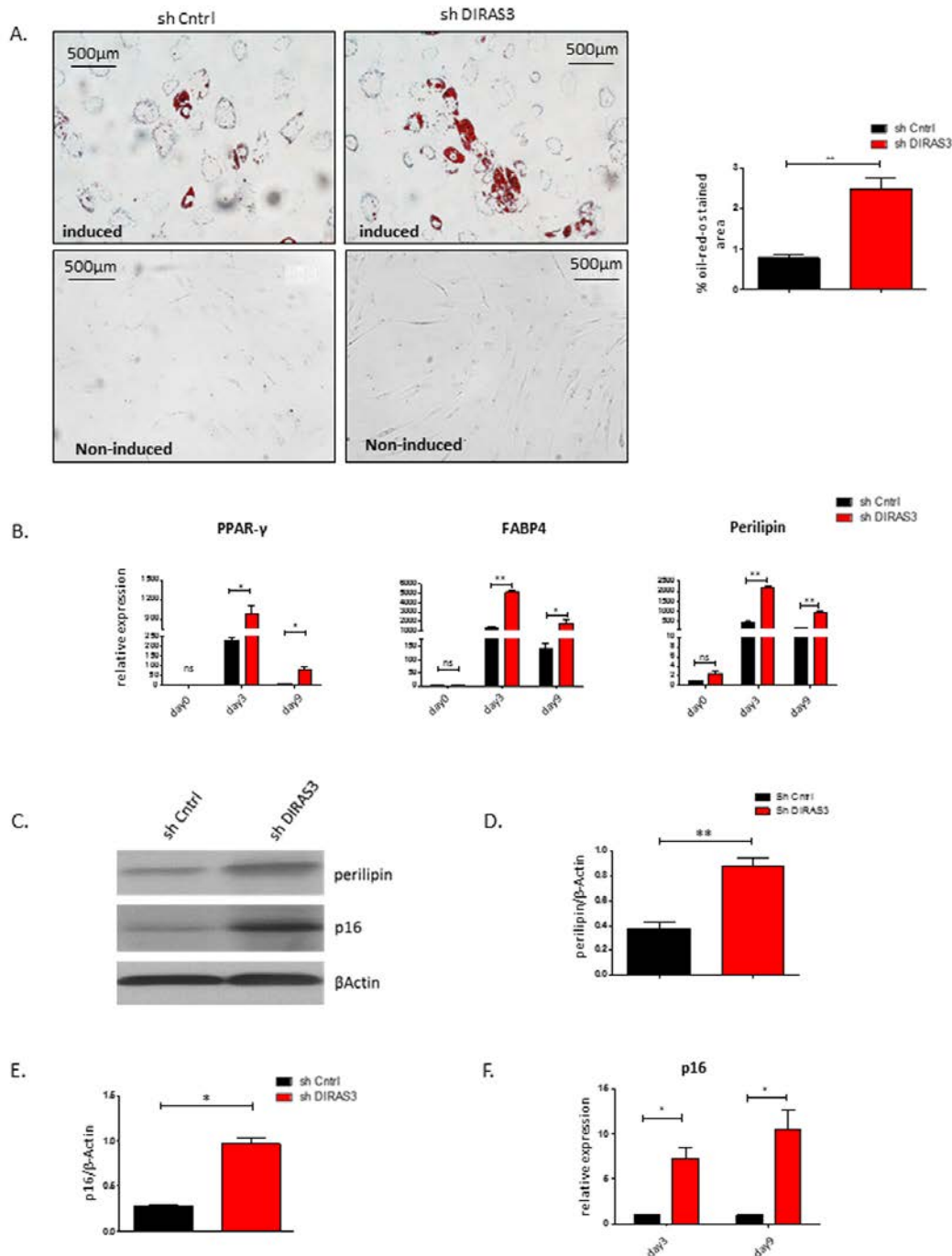


**Figure 6. Silencing of DIRAS3 in ASCs induces both premature senescence and adipogenic differentiation.** (A) (Left panel) Adipogenic differentiation of ASCs was estimated by staining the cells with Oil-Red-O stain at day 9 post induction of differentiation. Non-induced ASC controls are shown. (Right panel) Quantification of Oil-Red-O stained area using image J is shown (n=3). (B) Expression of PPAR $\gamma$ 2, FABP4 and Perilipin mRNA was estimated at day 3 and day 9 post induction of adipogenesis. Expression at day 0 before induction was taken as 1 and fold increase was calculated. Values are normalized to  $\beta$  Actin. (C) Perilipin and p16<sup>INK4A</sup> protein levels were analysed in DIRAS3 KD and control ASCs at day 9 post induction of adipogenesis by western blotting.  $\beta$ -Actin protein served as input control. (D and E) Densitometric evaluation of western blots bands from figure C. Fold changes in densitometric band intensities of perilipin (D) and p16<sup>INK4A</sup> (E) normalized to  $\beta$ -Actin protein, acquired by image J were plotted. (F) p16<sup>INK4A</sup> mRNA expression was analysed in DIRAS3 KD (red) and control ASCs (black) at day 3 and 9 post adipogenesis induction by q-RT\_PCR analysis. All error bars represents the means  $\pm$  SEM. p values \* = p<0.05, \*\* = p<0.001 and \*\*\* = p<.0001.

persistently activated (see [33] for a review). Thus, an appropriate intensity of growth-regulatory pathways, such as mTOR signaling, is important for decisions on given cell fates, such as self-renewal, proliferation, senescence and differentiation in adult stem/progenitor cells. Our findings are in keeping with this model. DIRAS3 silencing induced hyperactivity of mTOR promotes adipogenesis and premature senescence in human ASCs (this study, [14]). Rapamycin abrogates these effects. Similar data are available from other adult stem cell models. Epithelial stem cells undergo differentiation and senescence upon aberrant stimulation of mTOR [18], while reducing mTOR activity by rapamycin prevents senescence and terminal differentiation [30]. Aging adult muscle stem cells (MuSCs) can shift from a quiescent phenotype, which is crucial for transient amplification and self-renewal, to an over-activated phenotype characterized by increased activity of different signaling cascades that leads to premature senescence and terminal differentiation [34-36]. Moreover, mTOR acts as a regulator of the balance between quiescence, senescence and differentiation in neural stem cells [37, 38]. Precedence from work on MuSCs suggests that intrinsic mediators of stem cell quiescence exists, which can counteract the senescence program and promote self-renewal [39]. DIRAS3 as an intrinsic negative regulator of Akt-mTOR signaling may fulfill a similar function in ASCs, namely negative regulation of terminal adipogenic differentiation and senescence driven by stimulation of the Akt-mTOR pathway.

Senescent cells develop a SASP including chemo/cytokines with pro-inflammatory properties, which modulate tissue microenvironment and systemic phenotypes [31, 40]. The present study showed that DICS contributes to the manifestation of a SASP in ASCs and identified IL-8 as a specific factor up-regulated by DICS. It is interesting to note that IL-8 is specifically upregulated in senescent ASCs isolated from omental adipose biopsies of severe obese humans [17], because we previously identified DIRAS3 as a WL target gene in ASCs of formerly obese people [14]. We found no upregulation of IL-6, IL-1 $\beta$  and TNF  $\alpha$  by silencing of DIRAS3. Others have shown that for example IL-6 is increased in p16-positive cells isolated from inguinal adipose tissue of BubR1 progeroid mice [24]. Thus the composition of the SASP varies dependent on the senescent cell type, tissue and stress-inducing stimuli.

As mentioned above, ample evidence suggests that impaired replicative and adipogenic capacity are hallmarks of preadipocyte aging and adipogenesis is impaired in senescent ASCs. Senescent cells leave the

cell cycle with a permanent arrest in G0 and lose their ability to differentiate [19]. Our present study shows that silencing of DIRAS3 in human ASCs activates Akt-mTOR signaling and induces premature senescence. DIRAS3 KD induces however also adipogenesis and the resulting adipocyte population contains increased level of adipocyte and senescence markers. Moreover, we demonstrate that *in vitro* differentiated wild type adipocytes possess characteristics of adipocytes and senescence at the single cell level. This suggests that differentiating DIRAS3 KD ASCs and/or terminally differentiated adipocytes most likely acquire a senescence-like phenotype. Similar to our study it was shown that mature adipocytes of mice on a high-fat diet obtain key characteristics of senescence [16]. Moreover, other post-mitotic, terminally differentiated cells, which cannot re-enter the cell cycle, have also been found to develop characteristics of cellular senescence. This was shown for cardiac myocytes and neurons and is discussed as “senescent after differentiation”, a novel pathway to the formation of senescent cells [41].

The interaction between terminal differentiation and cellular senescence is poorly understood. Silencing of DIRAS3 in ASCs activates Rb induced cell cycle arrest. Rb plays a role in cellular senescence but also in several terminal differentiation programs of adult stem/progenitor cells [42]. Available data on adipogenesis are complicated. Studies in preadipocyte cell lines showed either activation [43] or repression of adipogenesis by Rb [44]. Moreover, Rb was shown to determine white versus beige adipocyte differentiation [45]. More work is necessary to better understand the signaling circuits down-stream of DIRAS3, which regulate adipogenesis and senescence.

Previous work from our group indicated that WL postpones the onset of replicative senescence in ASCs explanted from sWAT of formerly obese humans [10]. Subsequently we identified DIRAS3 as a WL target gene up-regulated in ASCs of sWAT of formerly obese people [14]. In combination with these studies, our present findings suggest that WL-induced upregulation of DIRAS3 reduces senescence and adipogenesis in ASCs of formerly obese people and promotes ASC self-renewal by restricting Akt-mTOR signaling. This is in keeping with the hypothesis that obesity-induced hyperactive Akt-mTOR signaling contributes to premature aging and reduced self-renewal capacity of ASCs while WL inhibits this pathway and hence protects ASCs.

In conclusion, the present study demonstrates a novel function of DIRAS3 in regulation of proliferation, senescence and differentiation of human ASCs.

**Table 1. Characteristics of the subjects participated in this study.**

n	Age (Years)	Weight	BMI
8	35 ± 12	65 ± 6	25 ± 4

All donors were healthy formerly obese Caucasian women, which underwent routine abdominoplasty after long-term weight-loss interventions. None of the women suffered from diabetes, liver, renal or other severe metabolic diseases. None of the women had cancer. Clinical and anthropometric parameters are indicated.

## METHODS

### Donors

Human sWAT samples were taken from eight formerly obese Caucasian women undergoing routine abdominoplasty after long-term weight loss interventions at the Institute for Plastic and Reconstructive Surgery (Medical University Innsbruck, Austria) [14, 46]. The patients gave their informed written consent and had been approved by the ethical committee of Innsbruck Medical University, Austria, according to the Declaration of Helsinki. None of the women suffered from diabetes, liver, renal or other severe metabolic diseases. None of the women had cancer. The clinical and anthropometric parameters are indicated in Table 1. The sWAT samples were taken from the lower abdomen (infraumbilical). The probes were exactly resected from the layer between fascia of scarpa and rectus fascia.

### Mouse Xenograft studies

Mice were treated in accordance with the guidelines of the “European Convention for the Protection of Vertebrate Animals used for Experimental and other Scientific Purposes” and the Austrian law. Animal experiments were approved by the ethics committee of the Austrian Federal Ministry of Science and Research (Application No. ZI. 188809/13). Six week old Crl:SHO-Prdke<sup>scid</sup>Hr<sup>hr</sup> female mice were purchased from Charles River (Germany). Human ASCs were infected with shCntrl or shDIRAS3 expressing lentiviruses. Cells were puromycin selected and 4 days later  $1.5 \times 10^5$  cells were injected subdermally into the flank of each mice (n=5 per group). Six weeks later, Forane® anesthetized mice were sacrificed and transplanted tissue site was surgically removed, fixed, paraffin embedded, sectioned and stained. Tissue sections were selected based on the hematoxylin and eosin stain. Antigen retrieval was performed by boiling in 6.5mM sodium citrate buffer (pH 6) for 10 min. 3%BSA/PBS was used for blocking. Sections were incubated at 4 °C overnight with anti p16<sup>INK4A</sup> antibody (1:50) (p16 (clone JC8), Santa Cruz). Anti-mouse

secondary Ab was applied for 1hr at room temperature. DAB chromogen was added for 1 min, washed followed by hematoxylin staining for 1 min and mounting. Number of p16 positive cells was counted per section.

### Isolation of ASCs from human subcutaneous adipose tissue and cell culture of ASCs

ASCs were isolated from abdominal sWAT samples obtained by incision from female donors undergoing elective plastic abdominal surgery essentially as described [5]. Briefly, after surgery adipose tissue biopsies were transferred into sterile serum-free ASC medium (DMEM/F-12 medium (1:1) with HEPES and L-glutamine (Gibco, Vienna, Austria), supplemented with 33 µM biotin, 17 µM pantothenate and 12.5 µg/ml gentamicin and processed in a laminar flow sterile work bench class II. After rinsing with sterile PBS fibrous material and blood vessels were dissected. The tissue was cut into pieces and digested by collagenase in digestion buffer (PBS containing 200 U/ml collagenase (CLS Type I, Worthington Biochemical Corp., Lakewood, NJ) and 2% w/v BSA). The cells were purified by centrifugation, filtration steps and erythrocyte lysis (erythrocyte lysis buffer was 0.155 M NH<sub>4</sub>Cl, 5.7 mM K<sub>2</sub>HPO<sub>4</sub>, 0.1 mM EDTA, pH 7.3). The isolated cells were referred to as stromal vascular fraction (SVF). Afterwards the cells of the SVF were suspended in ASC medium (DMEM/F-12 medium (1:1) with HEPES and L-glutamine (Gibco, Vienna, Austria) containing 33µM biotin, 17µM pantothenate and 12.5µg/ml gentamicin) supplemented with 10% FBS (Gibco, Vienna, Austria) and seeded into 6-well cell culture dishes at a density of 70 000 cells per cm<sup>2</sup>. Following 16 h of attachment, cells were kept for 6 days in serum-free ASC medium and non-adherent cells were continuously removed by washing. The remaining cell fraction was referred to as passage 1 (P1). These cells were then stored in liquid N<sub>2</sub>. After thawing cells were seeded overnight in ASC medium supplemented with 10% FBS, adherent cells were washed and cultivated in PM4 medium (ASC medium supplemented with 2.5 % FBS, 10 ng/ml EGF, 1 ng/ml bFGF, 500 ng/ml insulin). Cells were passaged at a ratio of 1:2 when they reached 70% confluence.

## Adipogenesis assay

ASCs were seeded at a density of 10,000 cells/cm<sup>2</sup> and grown till confluence in PM4 medium [47]. After a resting period of 48 hours in ASC medium (Dulbecco's modified Eagle medium/F-12 medium (1:1) with hydroxyethylpiperazineethanesulfonic acid and -glutamine (Gibco), supplemented with 33  $\mu$ M biotin, 17  $\mu$ M pantothenate, 12.5  $\mu$ g/mL gentamicin), adipogenesis was induced using differentiation medium (ASC medium supplemented with 0.2nM insulin (Roche, Vienna, Austria), 0.5mM 3-isobutyl-1-methylxanthine, 0.25  $\mu$ M dexamethasone, 2.5% fetal bovine serum, and 10  $\mu$ g/mL transferrin (Sigma, Vienna, Austria). After day 3 of differentiation, the medium was changed and the cells were cultivated in differentiation medium without 3-isobutyl-1-methylxanthine. For optical visualization of lipid droplets, cells were fixed with 4% paraformaldehyde in phosphate buffered saline (PBS) for 1 hour and stained with 0.3% Oil-Red-O (Sigma) in isopropanol/water (60:40) for 1 hour. Final washing procedure was carried out two times with H<sub>2</sub>O.

## Proliferation assay

0.5 $\times$ 10<sup>5</sup> differentially transduced cells were seeded in 6-well plates and proliferation of cells was monitored by counting the cells over a period of seven days from seeding.

## Colony formation assay

The colony formation assay was done as described [48]. Briefly, 500 cells either shDIRAS3 or shControl transduced were seeded in six well plates. After 10 days of culture colonies derived from single cells were fixed, stained with crystal violet and counted.

## CSFE proliferation assay

Assay was conducted as described [49]. Briefly, ACSs were infected with either shDIRAS3 or shControl expressing lentiviruses and selected using puromycin. Cells were stained with 1 $\mu$ M CFSE in PBS. Cells were incubated for 10min at 4°C and washed twice with 10%FCS/DMEM-F12 HAM to quench unbound CFSE and its deacetylated form. Followed by four days in culture CFSE signal was analyzed by FACS Canto (BD Biosciences).

## Retroviral gene expression system

The retroviral gene expression system used in the present study is described [14, 5]. DIRAS3 shRNA lentiviruses: sh1 (TRCN0000047771) and sh2

(TRCN0000047772) are from the shRNA set #RHS4533 for NM\_004675 from Open Biosystems, Vienna. In short, DIRAS3 shRNA and scrambled shRNA (sh Cntrl) cloned in pLKO.1 – TRC cloning vector [50] were purchased from Open Biosystems, Vienna. pLKO.1 empty vector was a gift from David Root (Addgene plasmid # 10878). These vectors were transformed and propagated in One Shot Stbl3 chemically competent *E. coli* (Invitrogen, USA). For lentivirus particle production each sh plasmid was separately co-transfected with packaging plasmid pMD2.G and psPAX2 (Addgene plasmids 12259 and 12260) into HEK293T cells, as described [5]. Briefly, 9 million HEK293T cells in 10 ml DMEM medium (Sigma) with 10 % FCS (Sigma, Vienna, Austria) were transfected with 4.4  $\mu$ g sh plasmid, 11  $\mu$ g psPAX2 and 3.6  $\mu$ g pMD2.G plasmid using 54  $\mu$ l Lipofectamine 2000 (Life Technologies). After 16 hours medium was replaced with 6 ml fresh DMEM medium containing 10 % FCS. After 48 hours virus particles were harvested by collecting the supernatant and centrifuging at 3000 rpm for 10 min. The supernatant was syringed filtered through 0.45 $\mu$ m filter, aliquoted and stored at -80°C. Transduction efficiency of lentiviruses in human ASCs was confirmed by transducing these cells with lentiviruses expressing GFP. The efficiency of infection was > 90 % (Supplementary Fig. S1C).

## SA- $\beta$ -Galactosidase staining of senescent cells

The senescent status of cells was verified by in situ staining for SA- $\beta$ -galactosidase, as described [29]. Briefly, cells grown on 9.6-cm<sup>2</sup> cell culture dishes were washed three times with PBS and fixed with 2% formaldehyde/0.8% glutaraldehyde in PBS. After washing with PBS, the cells were incubated in  $\beta$ -galactosidase staining solution (150mM NaCl, 2mM MgCl<sub>2</sub>, 5mM potassium ferricyanide, 5mM potassium ferrocyanide, 40mM citric acid, 12mM sodium phosphate, pH 6.0, containing 1mg/mL 5-bromo-4-chloro-3-indolyl- $\beta$ -d-galactoside (X-gal)) for 24 hours at 37°C. The reaction was stopped by washing in PBS. The fluorescence based SA- $\beta$ -Galactosidase staining assay was performed as described by [51]. Briefly, cells were incubated with 100nM bafilomycin A1 for 1 h to alkalize lysosomes. Cells were further incubated for 2 h with C<sub>12</sub>FDG at a final concentration of 33 $\mu$ M, trypsinized, washed and analyzed by FACS.

## Laser scanning confocal indirect immunofluorescence microscopy (IF-CLSM)

IF-CLSM was performed as described [5]. Antibodies against Ki - 67 (Neomarkers) and gamma H2A.X (Phospho S139) (Abcam) were used in combination with Alexa Fluor 488 goat anti rabbit and Alexa Fluor 488 donkey anti mouse (Invitrogen) antibodies.

**Table 2. The primer sequences used the present study are indicated.**

Gene	Direction	Sequence
βActin	Forward	AGAAAATCTGGCACACACC
	Reverse	AGAGGCGTACAGGGATAGCA
DIRAS3	Forward	CATAAGTTCCCCATCGTGCT
	Reverse	GAACAGCTCCTGCACATTCA
p16	Forward	CCCCACTACCGTAAATCTCCAT
	Reverse	CTGCCATTTGCTAGCAGTGTGACT
P21	Forward	AGACCAGCATGACAGATTTTC
	Reverse	ACTGAGACTAAGGCAGAAGA
IL-8	Forward	AAGGAAAACCTGGGTGCAGAG
	Reverse	ATTGCATCTGGCAACCCTAC
FABP4	Forward	CAGTGTGAATGGGGATGTGA
	Reverse	CGTGAAGTGACGCCTTT
PPARγ2	Forward	ATGGGTGAAACTCTGGGAGA
	Reverse	TGGAATGTCTTCGTAATGTGGA
Perilipin	Forward	GACAACGTGGTGGACACAGT
	Reverse	CTGGTGGGTTGTCGATGTC

### Quantitative RT PCR gene expression analysis

The method is described [5]. Primers sequences are shown in Table 2.

### Western blot analysis

Western blot analysis was performed as described [5]. Cell lysates were separated by SDS-PAGE and blotted on PVDF membranes. Following antibodies were used: Mouse anti human β-Actin, GAPDH (Ambion), CEBP-beta (C-19) (Santa Cruz), gamma H2A.X (Phospho S139) (Abcam), anti-mouse IgG HRP conjugate (Promega, Mannheim #W420B), donkey anti goat IgG-HRP (Promega, Mannheim #V805A), rabbit anti-rat IgG HRP (Dako Cytomation, Hamburg, #P0450), pP53, P53, pRb, Rb, pAkt (S473), Akt, pP70S6K (T389) and P70S6K, were from (Cell Signaling). Image J software was used for densitometric analyses.

### Flow cytometry analysis

Differentially transduced ASCs were incubated for 4 hrs with brefeldin A (5μg/ml), followed by fixation and permeabilization. Cells were stained by PerCP-Cy5.5-IL-8 antibody and analyzed by FACS using a

FACSCanto II (BD Biosciences). Data was analyzed employing FlowJo software.

### IL-8 ELISA

ELISA was performed following the protocol from Human IL-8 (2<sup>nd</sup> Generation) ELISA Ready-SET-Go kit (eBioscience Ref: 88-8086-22).

### Statistical Analysis

A statistical analysis was performed in GraphPad Prism (GraphPad Software Inc., La Jolla, CA, USA). The significance of difference between means was assessed by Student's t test or analysis of variance (ANOVA). Error bars are represented as the mean ± SEM.

### AUTHOR CONTRIBUTIONS

MM provided sWAT probes. AE, MM and WZ designed experiments. AE and WZ performed data analysis. AE performed the experiments and contributed to writing of the manuscript. WZ conceived the study and wrote the manuscript. All authors read and approved the manuscript.

## ACKNOWLEDGMENTS

This work was supported by intramural funding from the University of Innsbruck.

## CONFLICTS OF INTEREST

The authors declare no conflict of interest.

## REFERENCES

1. Zeve D, Tang W, Graff J. Fighting fat with fat: the expanding field of adipose stem cells. *Cell Stem Cell*. 2009; 5:472–81. doi: 10.1016/j.stem.2009.10.014
2. Rodeheffer MS, Birsoy K, Friedman JM. Identification of white adipocyte progenitor cells in vivo. *Cell*. 2008; 135:240–49. doi: 10.1016/j.cell.2008.09.036
3. Tang W, Zeve D, Suh JM, Bosnakovski D, Kyba M, Hammer RE, Tallquist MD, Graff JM. White fat progenitor cells reside in the adipose vasculature. *Science*. 2008; 322:583–86. doi: 10.1126/science.1156232
4. Zuk PA, Zhu M, Mizuno H, Huang J, Futrell JW, Katz AJ, Benhaim P, Lorenz HP, Hedrick MH. Multilineage cells from human adipose tissue: implications for cell-based therapies. *Tissue Eng*. 2001; 7:211–28. doi: 10.1089/107632701300062859
5. Mitterberger MC, Lechner S, Mattesich M, Kaiser A, Probst D, Wenger N, Pierer G, Zwerschke W. DLK1(PREF1) is a negative regulator of adipogenesis in CD105+/CD90+/CD34+/CD31–/FABP4– adipose-derived stromal cells from subcutaneous abdominal fat pats of adult women. *Stem Cell Res (Amst)*. 2012; 9:35–48. doi: 10.1016/j.scr.2012.04.001
6. Cawthorn WP, Scheller EL, MacDougald OA. Adipose tissue stem cells meet preadipocyte commitment: going back to the future. *J Lipid Res*. 2012; 53:227–46. doi: 10.1194/jlr.R021089
7. Cristancho AG, Lazar MA. Forming functional fat: a growing understanding of adipocyte differentiation. *Nat Rev Mol Cell Biol*. 2011; 12:722–34. doi: 10.1038/nrm3198
8. MacLean PS, Higgins JA, Giles ED, Sherk VD, Jackman MR. The role for adipose tissue in weight regain after weight loss. *Obes Rev*. 2015 (Suppl 1); 16:45–54. doi: 10.1111/obr.12255
9. Lam YY, Ghosh S, Civitarese AE, Ravussin E. Six-month calorie restriction in overweight individuals elicits transcriptomic response in subcutaneous adipose tissue that is distinct from effects of energy deficit. *J Gerontol A Biol Sci Med Sci*. 2016; 71:1258–65. doi: 10.1093/gerona/glv194
10. Mitterberger MC, Mattesich M, Zwerschke W. Bariatric surgery and diet-induced long-term caloric restriction protect subcutaneous adipose-derived stromal/progenitor cells and prolong their life span in formerly obese humans. *Exp Gerontol*. 2014; 56:106–13. doi: 10.1016/j.exger.2014.03.030
11. Pérez LM, Suárez J, Bernal A, de Lucas B, San Martín N, Gálvez BG. Obesity-driven alterations in adipose-derived stem cells are partially restored by weight loss. *Obesity (Silver Spring)*. 2016; 24:661–69. doi: 10.1002/oby.21405
12. Yu Y, Luo R, Lu Z, Wei Feng W, Badgwell D, Issa JP, Rosen DG, Liu J, Bast RC Jr. Biochemistry and biology of ARHI (DIRAS3), an imprinted tumor suppressor gene whose expression is lost in ovarian and breast cancers. *Methods Enzymol*. 2006; 407:455–68. doi: 10.1016/S0076-6879(05)07037-0
13. Lu Z, Luo RZ, Lu Y, Zhang X, Yu Q, Khare S, Kondo S, Kondo Y, Yu Y, Mills GB, Liao WS, Bast RC Jr. The tumor suppressor gene ARHI regulates autophagy and tumor dormancy in human ovarian cancer cells. *J Clin Invest*. 2008; 118:3917–29.
14. Ejaz A, Mitterberger MC, Lu Z, Mattesich M, Zwierzina ME, Hörl S, Kaiser A, Viertler HP, Rostek U, Meryk A, Khalid S, Pierer G, Bast RC Jr, Zwerschke W. Weight loss upregulates the small GTPase DIRAS3 in human white adipose progenitor cells, which negatively regulates adipogenesis and activates autophagy via Akt–mTOR inhibition. *EBioMedicine*. 2016; 6:149–61. doi: 10.1016/j.ebiom.2016.03.030
15. Laplante M, Sabatini DM. mTOR signaling in growth control and disease. *Cell*. 2012; 149:274–93. doi: 10.1016/j.cell.2012.03.017
16. Minamino T, Orimo M, Shimizu I, Kunieda T, Yokoyama M, Ito T, Nojima A, Nabetani A, Oike Y, Matsubara H, Ishikawa F, Komuro I. A crucial role for adipose tissue p53 in the regulation of insulin resistance. *Nat Med*. 2009; 15:1082–87. doi: 10.1038/nm.2014
17. Roldan M, Macias-Gonzalez M, Garcia R, Tinahones FJ, Martin M. Obesity short-circuits stemness gene network in human adipose multipotent stem cells. *FASEB J*. 2011; 25:4111–26. doi: 10.1096/fj.10-171439
18. Castilho RM, Squarize CH, Chodosh LA, Williams BO, Gutkind JS. mTOR mediates Wnt-induced epidermal stem cell exhaustion and aging. *Cell Stem Cell*. 2009; 5:279–89. doi: 10.1016/j.stem.2009.06.017

19. van Deursen JM. The role of senescent cells in ageing. *Nature*. 2014; 509:439–46. doi: 10.1038/nature13193
20. Serrano M, Lin AW, McCurrach ME, Beach D, Lowe SW. Oncogenic ras provokes premature cell senescence associated with accumulation of p53 and p16INK4a. *Cell*. 1997; 88:593–602. doi: 10.1016/S0092-8674(00)81902-9
21. Chen Z, Trotman LC, Shaffer D, Lin HK, Dotan ZA, Niki M, Koutcher JA, Scher HI, Ludwig T, Gerald W, Cordon-Cardo C, Pandolfi PP. Crucial role of p53-dependent cellular senescence in suppression of Pten-deficient tumorigenesis. *Nature*. 2005; 436:725–30. doi: 10.1038/nature03918
22. Acosta JC, O’Loughlen A, Banito A, Guijarro MV, Augert A, Raguz S, Fumagalli M, Da Costa M, Brown C, Popov N, Takatsu Y, Melamed J, d’Adda di Fagagna F, et al. Chemokine signaling via the CXCR2 receptor reinforces senescence. *Cell*. 2008; 133:1006–18. doi: 10.1016/j.cell.2008.03.038
23. Baker DJ, Perez-Terzic C, Jin F, Pitel KS, Niederländer NJ, Jeganathan K, Yamada S, Reyes S, Rowe L, Hiddinga HJ, Eberhardt NL, Terzic A, van Deursen JM. Opposing roles for p16Ink4a and p19Arf in senescence and ageing caused by BubR1 insufficiency. *Nat Cell Biol*. 2008; 10:825–36. doi: 10.1038/ncb1744
24. Baker DJ, Wijshake T, Tchkonja T, LeBrasseur NK, Childs BG, van de Sluis B, Kirkland JL, van Deursen JM. Clearance of p16Ink4a-positive senescent cells delays ageing-associated disorders. *Nature*. 2011; 479:232–36. doi: 10.1038/nature10600
25. Xu M, Palmer AK, Ding H, Weivoda MM, Pirtskhalava T, White TA, Sepe A, Johnson KO, Stout MB, Giorgadze N, Jensen MD, LeBrasseur NK, Tchkonja T, Kirkland JL. Targeting senescent cells enhances adipogenesis and metabolic function in old age. *Elife*. 2015; 19;4:e12997. doi: 10.7554/eLife.12997.
26. Baker DJ, Childs BG, Durik M, Wijers ME, Sieben CJ, Zhong J, Saltness RA, Jeganathan KB, Verzosa GC, Pezeshki A, Khazaie K, Miller JD, van Deursen JM. Naturally occurring p16(Ink4a)-positive cells shorten healthy lifespan. *Nature*. 2016; 530:184–89. doi: 10.1038/nature16932
27. Kirkland JL, Dobson DE. Preadipocyte function and aging: links between age-related changes in cell dynamics and altered fat tissue function. *J Am Geriatr Soc*. 1997; 45:959–67. doi: 10.1111/j.1532-5415.1997.tb02967.x
28. Park JS, Kim HY, Kim HW, Chae GN, Oh HT, Park JY, Shim H, Seo M, Shin EY, Kim EG, Park SC, Kwak SJ. Increased caveolin-1, a cause for the declined adipogenic potential of senescent human mesenchymal stem cells. *Mech Ageing Dev*. 2005; 126:551–59. doi: 10.1016/j.mad.2004.11.014
29. Mitterberger MC, Lechner S, Mattesich M, Zwerschke W. Adipogenic differentiation is impaired in replicative senescent human subcutaneous adipose-derived stromal/progenitor cells. *J Gerontol A Biol Sci Med Sci*. 2014; 69:13–24. doi: 10.1093/gerona/glt043
30. Iglesias-Bartolome R, Patel V, Cotrim A, Leelahavanichkul K, Molinolo AA, Mitchell JB, Gutkind JS. mTOR inhibition prevents epithelial stem cell senescence and protects from radiation-induced mucositis. *Cell Stem Cell*. 2012; 11:401–14. doi: 10.1016/j.stem.2012.06.007
31. Malaquin N, Martinez A, Rodier F. Keeping the senescence secretome under control: molecular reins on the senescence-associated secretory phenotype. *Exp Gerontol*. 2016; 82:39–49. doi: 10.1016/j.exger.2016.05.010
32. Borkan GA, Hulst DE, Gerzof SG, Robbins AH, Silbert CK. Age changes in body composition revealed by computed tomography. *J Gerontol*. 1983; 38:673–77. doi: 10.1093/geronj/38.6.673
33. Iglesias-Bartolome R, Gutkind JS. Signaling circuitries controlling stem cell fate: to be or not to be. *Curr Opin Cell Biol*. 2011; 23:716–23. doi: 10.1016/j.ceb.2011.08.002
34. Bernet JD, Doles JD, Hall JK, Kelly Tanaka K, Carter TA, Olwin BB. p38 MAPK signaling underlies a cell-autonomous loss of stem cell self-renewal in skeletal muscle of aged mice. *Nat Med*. 2014; 20:265–71. doi: 10.1038/nm.3465
35. Cosgrove BD, Gilbert PM, Porpiglia E, Mourkioti F, Lee SP, Corbel SY, Llewellyn ME, Delp SL, Blau HM. Rejuvenation of the muscle stem cell population restores strength to injured aged muscles. *Nat Med*. 2014; 20:255–64. doi: 10.1038/nm.3464
36. Sousa-Victor P, Gutarra S, García-Prat L, Rodríguez-Ubreva J, Ortet L, Ruiz-Bonilla V, Jardí M, Ballestar E, González S, Serrano AL, Perdiguero E, Muñoz-Cánoves P. Geriatric muscle stem cells switch reversible quiescence into senescence. *Nature*. 2014; 506:316–21. doi: 10.1038/nature13013
37. Paliouras GN, Hamilton LK, Aumont A, Joppé SE, Barnabé-Heider F, Fernandes KJ. Mammalian target of rapamycin signaling is a key regulator of the transit-amplifying progenitor pool in the adult and aging forebrain. *J Neurosci*. 2012; 32:15012–26. doi: 10.1523/JNEUROSCI.2248-12.2012



38. Schneider L, Pellegatta S, Favaro R, Pisati F, Roncaglia P, Testa G, Nicolis SK, Finocchiaro G, d'Adda di Fagagna F. DNA damage in mammalian neural stem cells leads to astrocytic differentiation mediated by BMP2 signaling through JAK-STAT. *Stem Cell Rep.* 2013; 1:123–38. doi: 10.1016/j.stemcr.2013.06.004
39. Chakkalakal JV, Jones KM, Basson MA, Brack AS. The aged niche disrupts muscle stem cell quiescence. *Nature.* 2012; 490:355–60. doi: 10.1038/nature11438
40. Coppé JP, Desprez PY, Krtolica A, Campisi J. The senescence-associated secretory phenotype: the dark side of tumor suppression. *Annu Rev Pathol.* 2010; 5:99–118. doi: 10.1146/annurev-pathol-121808-102144
41. Naylor RM, Baker DJ, van Deursen JM. Senescent cells: a novel therapeutic target for aging and age-related diseases. *Clin Pharmacol Ther.* 2013; 93:105–16. doi: 10.1038/clpt.2012.193
42. Sage J. The retinoblastoma tumor suppressor and stem cell biology. *Genes Dev.* 2012; 26:1409–20. doi: 10.1101/gad.193730.112
43. Chen PL, Riley DJ, Chen Y, Lee WH. Retinoblastoma protein positively regulates terminal adipocyte differentiation through direct interaction with C/EBPs. *Genes Dev.* 1996; 10:2794–804. doi: 10.1101/gad.10.21.2794
44. Fajas L, Egler V, Reiter R, Hansen J, Kristiansen K, Debril MB, Miard S, Auwerx J. The retinoblastoma-histone deacetylase 3 complex inhibits PPAR $\gamma$  and adipocyte differentiation. *Dev Cell.* 2002; 3:903–10. doi: 10.1016/S1534-5807(02)00360-X
45. Hansen JB, Jørgensen C, Petersen RK, Hallenborg P, De Matteis R, Bøye HA, Petrovic N, Enerbäck S, Nedergaard J, Cinti S, te Riele H, Kristiansen K. Retinoblastoma protein functions as a molecular switch determining white versus brown adipocyte differentiation. *Proc Natl Acad Sci USA.* 2004; 101:4112–17. doi: 10.1073/pnas.0301964101
46. Mitterberger MC, Mattesich M, Klaver E, Lechner S, Engelhardt T, Larcher L, Pierer G, Piza-Katzer H, Zwerschke W. Adipokine profile and insulin sensitivity in formerly obese women subjected to bariatric surgery or diet-induced long-term caloric restriction. *J Gerontol A Biol Sci Med Sci.* 2010; 65:915–23. doi: 10.1093/gerona/g1q107
47. Lechner S, Mitterberger MC, Mattesich M, Zwerschke W. Role of C/EBP $\beta$ -LAP and C/EBP $\beta$ -LIP in early adipogenic differentiation of human white adipose-derived progenitors and at later stages in immature adipocytes. *Differentiation.* 2013; 85:20–31. doi: 10.1016/j.diff.2012.11.001
48. Zwierzina ME, Ejaz A, Bitsche M, Blumer M, Mitterberger MC, Mattesich M, Kaiser A, Pechriggl EJ, Hörl S, Pierer G, Rostek U, Fritsch H, Zwerschke W. Characterization of DLK1(PREF1)+/CD34+ progenitor cells in human white adipose tissues. *Stem Cell Res (Amst).* 2015; 15:403–18. doi: 10.1016/j.scr.2015.08.004
49. Urbani S, Caporale R, Lombardini L, Bosi A, Saccardi R. Use of CFDA-SE for evaluating the in vitro proliferation pattern of human mesenchymal stem cells. *Cytotherapy.* 2006; 8:243–53. doi: 10.1080/14653240600735834
50. Moffat J, Grueneberg DA, Yang X, Kim SY, Kloepper AM, Hinkle G, Piqani B, Eisenhaure TM, Luo B, Grenier JK, Carpenter AE, Foo SY, Stewart SA, et al. A lentiviral RNAi library for human and mouse genes applied to an arrayed viral high-content screen. *Cell.* 2006; 124:1283–98. doi: 10.1016/j.cell.2006.01.040
51. Debacq-Chainiaux F, Erusalimsky JD, Campisi J, Toussaint O. Protocols to detect senescence-associated beta-galactosidase (SA-beta-gal) activity, a biomarker of senescent cells in culture and in vivo. *Nat Protoc.* 2009; 4:1798–806. doi: 10.1038/nprot.2009.191